

Statistical product distributions for ultracold reactions in external fields

Maykel L. González-Martínez* and Olivier Dulieu
*Laboratoire Aimé Cotton, CNRS, Université Paris-Sud, ENS Cachan,
 Bât. 505, Campus d'Orsay, 91405 Orsay, France*

Pascal Larrégaray and Laurent Bonnet
Institut des Sciences Moléculaires, CNRS, Université Bordeaux 1, UMR 5255, 33405 Talence, France
 (Dated: October 21, 2014)

The main limitation of most ultracold chemistry studies to date is the lack of an analysis of reaction products. Here, we discuss the first generally tractable, rigorous theoretical framework for computing statistical product-state distributions for ultracold reactions in external fields. We show that fields have two main effects on the products of a statistical reaction, by: (1) modifying the product energy levels thus potentially reshaping the product distributions; and/or (2) adding or removing product states by changing the reaction exothermicity. By analyzing these effects and the strength of the formalism to distinguish between different reaction mechanisms in benchmark reactions involving ^{40}K and ^{87}Rb species, we argue that statistical predictions will help understanding product formation and control, and lead developments to realize the full potential of ultracold chemistry.

PACS numbers: 34.50.Cx, 34.50.Lf, 82.20.Bc

I. INTRODUCTION

Recent advances in producing and trapping species at temperatures below 1 mK have made ultracold chemistry a reality. For the first time, reactions can be explored in the fully quantum regime where resonances, tunneling, quantum degeneracy and other non-classical effects dominate the reaction dynamics. In addition, external fields may be used to favor or disfavor typical and exotic reaction mechanisms thus allowing their scrutiny with unprecedented detail, to “tailor” interactions and study the consequences of confinement upon reactivity. Fields can also be used to trap the ultracold species, drastically enhancing interrogation times and making it possible to probe the effects of the weakest interactions. Since 2010, pioneering experiments at JILA, Colorado, started addressing many of these issues in reactions involving mixed ultracold samples of K, Rb and KRb [1–3] by inferring reaction rates through the measurement of reactants losses.

Despite all key findings at JILA, and being commonly acknowledged as one of the most important applications for ultracold species [4, 5], low-temperature chemical reactions are most often considered for their role as *obstacles* to the stability of quantum gases [6–9]. This seems natural, since the main current experimental focus is on the production of ultracold molecules which reactions obstruct. Nevertheless, the problem of reaction rates and their dependence on external fields have attracted much interest; Quémener and Bohn [2, 3, 10, 11], Idziaszek, Julianne *et al.* [12–14], and Gao [15, 16] developed quantum models to interpret the rates measured at JILA, and discussed “universal” features in ultracold reactions.

Yet, the study of a chemical reaction goes necessarily beyond a description of its rate into that of its products:

The question of product-state distributions and state-to-state cross sections is among the biggest experimental and theoretical challenges in the field, with the potential to bring ultracold physics into the realm of chemistry [5]. Product distributions are far more sensitive than reaction rates to finer details of the dynamics, and would provide an integral view and deeper understanding of the underlying physics. In addition, even if neutral products are quite difficult to detect, ionic products may be more easily monitored in experiments on ultracold ion-neutral [17] or Penning-ionization reactions [18], and aid understanding radiative molecular formation, charge transfer and several other mechanisms. The issue seems specially timely for the first product distributions were very recently measured for the closely related process of 3-body recombination in an ultracold atomic gas [19].

A theory that accounts for external fields is essential as these are ubiquitous in ultracold experiments: fields are used for trapping the (ultra)cold species and/or controlling their interactions. In principle, a full description of low-temperature reactions can be derived from the quantum formalism for chemical reactions in electromagnetic fields developed by Tscherbul and Krems [20]. However, such rigorous quantum-mechanical calculations are not currently tractable for most cases of experimental interest. This is partly due to the huge number of rovibrational states involved in low-temperature collisions of relatively heavy species [21, 22]. There is, however, a more fundamental reason for this: Ultracold reactions span the most widely-different energy, length and time scales explored in chemistry to date, and hence pose an unprecedented challenge to chemical collision theory.

Nonetheless, Mayle and coworkers [21, 22] have shown that total reaction rates, and answers to a number of important questions regarding the statistics of global properties of such processes, may still be inferred using arguments from Rice-Ramsperger-Kassel-Marcus (RRKM)

* maykel.gonzalez-martinez@u-psud.fr

theory, the random matrix theory of nuclear scattering, and multichannel quantum defect theory (MQDT). The first empirical indication of such statistical behavior was recently reported for ultracold collisions of Er atoms [23].

In this paper, we set up the first theoretical framework for calculating statistical product-state distributions and state-to-state cross sections for ultracold reactions in external fields, by connecting traditional statistical theories [24, 25] and ultracold collision theory [26]. We show that such product distributions may be used as benchmarks for the founding assumptions of the theory, and hence provide fundamental tests for the statistical arguments of Mayle *et al.* [21, 22]. Moreover, they allow us to critically evaluate possible departures from statistical behavior, both qualitatively and quantitatively, being thus a powerful tool to rationalize any kind of reaction.

II. THEORY

A. Statistical formalism in external fields

We consider a reactive collision between two species, M_1^α and M_2^α , which yields two products, M_1^β and M_2^β , in the presence of an external field. Here, α and β loosely refer to reactants and products; in what follows, α is also used to represent the set of quantum numbers needed to specify the internal states of the reactants, while β is its analogous for the products.

Product-state distributions are obtained from the reaction cross section σ_r , with the probability density associated to an observable X , $\mathcal{P}(X) = \frac{1}{\sigma_r} \frac{\partial \sigma_r}{\partial X}$ [27]. In general, the only conserved quantity in an external field is the projection of the total angular momentum on the field axis, M , and the total reaction cross section can be obtained by adding all contributions from state-to-state cross sections, $\sigma_r = \sum_{M\alpha\beta} \sigma_{\alpha\rightarrow\beta}^M$. The rigorous quantum-mechanical expression for the state-to-state cross section from reactant state α to product state β , at a given M , energy E and field strength F is [20]

$$\sigma_{\alpha\rightarrow\beta}^M(E, F) = \frac{\pi \hbar^2 g_\alpha}{2\mu_\alpha(E - E_\alpha)} \times \sum_{L_\alpha M_{L_\alpha}} \sum_{L_\beta M_{L_\beta}} \left| S_{\alpha L_\alpha M_{L_\alpha}; \beta L_\beta M_{L_\beta}}^M(E, F) \right|^2 \quad (1)$$

where g_α is a degeneracy factor that equals 2 if the reactants are indistinguishable and 1 otherwise, μ_α is the reactants' reduced mass, E_α (E_β) is the species energy in state α (β), and L_α (L_β) is the space-fixed orbital angular momentum of the reactants (products) with projection M_{L_α} (M_{L_β}) on the field axis. The sums over the absolute squares of S -matrix elements define the transition probability $P_{\alpha\rightarrow\beta}^M$ from state α to β . Our model becomes *statistical* for we assume that reaction always proceeds through complex formation, whose dynamics renders the reactant and product channels statistically independent.

Following Hauser and Feshbach [24], or Miller [25]

$$P_{\alpha\rightarrow\beta}^M \approx p_\alpha^M p_\beta^M / \sum_\gamma p_\gamma^M, \quad (2)$$

where the explicit dependence on E and F has been omitted, as in what follows. The p^M quantities are capture probabilities—*i.e.*, the probability of complex formation, for a given M , when the species collide in a specific state. The sum in the denominator runs over all energetically accessible reactant and product channels, hence the ratio $p_\beta^M / \sum_\gamma p_\gamma^M$ is the fraction of collision complexes that dissociate into product state β . Eq. (2) is statistical for all capture probabilities are considered uncorrelated and is seen to satisfy the principle of detailed balance. In a further approximation, our reasoning may be extended to include inelastic processes, thus treating all *quenching* events statistically—although nonreactive scattering is less likely to involve complex formation.

A distinctive feature of ultracold experiments is the possibility to fully control the reactants' initial states, thus we fix α in what follows. The statistical state-to-state reaction cross section may be written as

$$\sigma_{\alpha\rightarrow\beta, r} = \frac{\pi \hbar^2 g_\alpha}{2\mu_\alpha(E - E_\alpha)} \sum_M p_\alpha^M \frac{p_\beta^M}{\sum_\gamma p_\gamma^M}, \quad (3)$$

from which the total reaction cross section $\sigma_{\alpha, r}$ is found by summing over all possible product states β , and the related total reaction rate $k_{\alpha, r} \equiv [2(E - E_\alpha)/\mu_\alpha]^{1/2} \sigma_{\alpha, r}$. Quantities for a specific temperature are obtained by averaging over the corresponding Boltzmann distribution. If reaction occurs, the probability density corresponding to an observable X in the products reads

$$\mathcal{P}_\alpha(X) = \left(\sum_M p_\alpha^M \frac{\sum_\beta p_\beta^M}{\sum_\gamma p_\gamma^M} \right)^{-1} \left(\sum_M p_\alpha^M \frac{\sum_\beta \frac{\partial p_\beta^M}{\partial X}}{\sum_\gamma p_\gamma^M} \right), \quad (4)$$

where the first term in parenthesis acts like a proportionality constant. The form of this distribution is readily visualized by recognizing that the sum over partial derivatives $\sum_\beta (\partial p_\beta^M / \partial X) = \delta(X) \sum_{\beta \in \{X\}} p_\beta^M$, where $\delta(X)$ is a Dirac δ -function and the sum includes only product states compatible with the value X . Contributions from different M values combine with different relative weights that approach the capture probabilities in the entrance channels if many product states are available.

Equations (3) and (4) provide detailed statistical predictions for the observables of a chemical reaction in an external field. In the ultracold regime, kinetic energies in the entrance/elastic (and possibly inelastic) channels are extremely low, hence a quantum-mechanical description is crucial for calculating the corresponding capture probabilities. By comparison, the kinetic energies available to the products are much larger and a simpler (semi)classical description should be appropriate. The issue of capture in the ultracold entrance channels has

received much attention in the last few years, mainly to describe the loss rates measured at JILA; various models have been proposed [1–3, 10, 12, 14, 15, 28, 29] that are valid under specific conditions. In addition, we have extended time-independent [30, 31] and time-dependent methods [32], and a variety of semiclassical and classical models, to make it possible to evaluate capture probabilities in external fields also for reactions at higher temperatures [33]. The statistical formalism is quite flexible as capture models may be chosen among all of the above, or new models developed, depending on the conditions of the experiment and desired level of sophistication.

B. Implementation details

The calculations for Eqs. (3) and (4) are performed in two main steps, which are described below.

First, quantum states are defined for all reactants and products by diagonalizing the Hamiltonians of the corresponding isolated species. For each species M_k^γ , every such state is associated an energy $E_{\gamma,k}$ and projection of the total angular momentum $m_{\gamma,k}$. Quantum numbers/labels are additionally associated to each state from the eigenfunction(s) with the largest contribution in the chosen basis—which are later used to produce quantum-state/label distributions. In addition, effective electric dipole moments are obtained for each state from the expectation value of the electric dipole operator.

Secondly, for each projection of the total angular momentum M , a capture probability p_γ^M is calculated for every combination of reactant/product states that satisfies: (1) it corresponds to an asymptotically open channel, $E \geq E_{\gamma,1} + E_{\gamma,2}$; and (2) the projection of the total angular momentum is conserved, $M = m_{\alpha,1} + m_{\alpha,2} + M_{L_\alpha} = m_{\beta,1} + m_{\beta,2} + M_{L_\beta}$. The latter involves completing the definition of channels by adding an orbital angular momentum L_γ , and associated projections $M_{L_\gamma} = -L_\gamma, \dots, L_\gamma$, to each combination of reactants/products states. In the case where only magnetic fields are present, an additional constraint is imposed based on the conservation of the total parity—calculated for each channel by multiplying the parities of the individual species (computed in the first step) and $(-1)^{L_\gamma}$. The capture models are chosen on the basis of the physical context and open channels are added until convergence is achieved. This whole step is repeated until convergence is achieved with respect to M .

III. RESULTS AND DISCUSSION

To illustrate our formalism, we focus on benchmark ultracold exoergic reactions involving ^{40}K , ^{87}Rb and their diatomic combinations. Reactive collisions between these species are barrierless, with exothermicities ΔE ranging from about 10 to 200 cm^{-1} , and proceeding through wells up to 8,000 cm^{-1} deep [7, 34]. Such large energy dif-

ferences are usually an indication of strong interactions among internal degrees of freedom (DOFs) of the intermediate complex. Strong interactions, a large number of states associated to the intermediate complex and a relatively few open exit channels most often lead to long-lived intermediates and statistical behavior. These are also the conditions for ergodic dynamics in classical phase space, recently studied by Croft and Bohn in ultracold molecular collisions [35].

Quantum states are computed with the Hamiltonians and parameters in Refs. [36–38]. Capture probabilities in the entrance channels are evaluated with a Wentzel-Kramers-Brillouin (WKB) tunneling model for reactions in magnetic fields, and the adiabatic variant of the quantum threshold model (QTM) [10] for those in electric fields. A semiclassical model based on phase-space theory (PST) [39–42], suitable to account for long-range dispersion interactions, *cf.*, Refs. [43–47], is used for capture probabilities from the products. In general, capture in barrierless reactions is dominated by long-range interactions, which are accounted for by the chosen models. Nevertheless, if necessary, short-range effects can be included in the statistical formalism by calculating capture probabilities using, *e.g.*, a quantum-mechanical [30, 32] or quasi-classical approach [48]; such studies require a detailed knowledge of the interaction potentials, which usually involve computationally expensive *ab initio* calculations. Further details are described in the Appendix.

A. Global properties

We first consider *global* properties, and remark an important consequence of summing over β in Eq. (3): In the common case where many more product than reactant states are available, $\sum_\beta p_\beta^M / \sum_\gamma p_\gamma^M \rightarrow 1$, and global quantities depend exclusively on the capture probabilities for the *entrance* channels. Such observables thus provide a “one-sided” description of the process and its governing dynamics, and contain no information on how (or even which) products are formed in the reaction.

In cases with many more product than reactant states, statistical predictions will be similar to those based on the “universal” assumption [12]—in which the wavefunction is considered to be fully absorbed once the short-range, chemical region is reached. However, statistical and universal predictions are not necessarily indistinguishable. For instance, ultracold isotopic-substitution reactions would have very small exothermicities and only a few available product states, thus global statistical and universal predictions could differ. Moreover, the requirement for universality implies nothing about the intermediate dynamics thus universal product distributions (not derivable from the “universal” methodology at present) would not necessarily agree with statistical predictions: The statistical assumption imposes a more stringent constraint, namely that capture probabilities in the entrance and product channels are statistically independent.

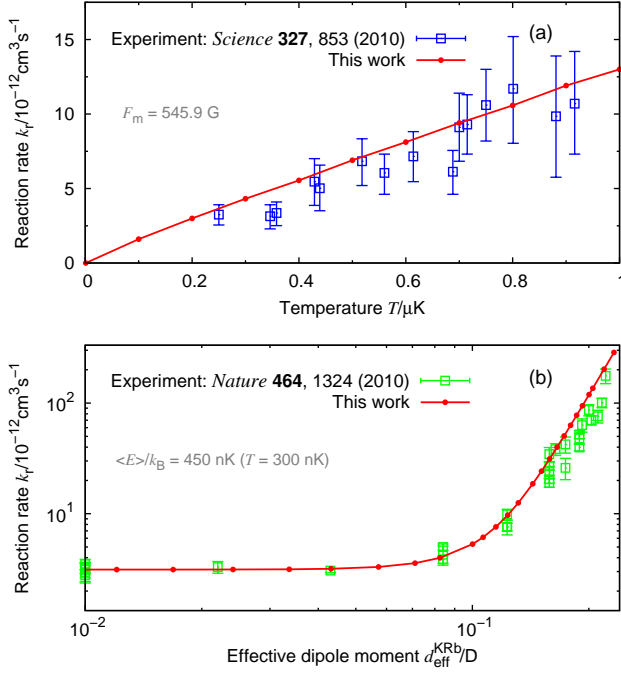


FIG. 1. (Color online) Experimental and statistical rates for ultracold reactions between ground-state $^{40}\text{K}^{87}\text{Rb}$ molecules in: (a) magnetic, F_m , and (b) electric, F_e , fields ($d_{\text{eff}}^{\text{KRb}} \propto F_e$).

Figure 1 shows experimental and statistical rates for ultracold reactions between two ground-state $^{40}\text{K}^{87}\text{Rb}$ molecules in magnetic and electric fields. Following our previous discussion, the statistical predictions correspond to those of the WKB and QTM models [1, 2, 12] chosen to evaluate capture probabilities in the entrance channel(s). The agreement between experimental and statistical predictions is hence a consequence of the success of these models to account for quantum effects in reactions of *undistinguishable fermions* such as $^{40}\text{K}^{87}\text{Rb}$. Because of Fermi statistics, such collisions can only occur with odd partial waves ($L_\alpha = 1, 3, \dots$) thus capture in the ultracold channels occurs via tunneling through dynamical barriers [1–3]. These barriers can be reshaped with applied electric fields, which induce long-range anisotropic dipolar interactions and lead to different tunneling probabilities for different M (M_{L_α}) values [2, 3, 10]. As shown in Fig. 1, field effects may induce striking order-of-magnitude variations in ultracold reaction rates.

It is important to note that quantitative agreement between theoretical and experimental rates, although a necessary condition, is *not* conclusive evidence on the statistical nature of a reaction. Within capture theory, capture in the entrance channels determines the rates in *any* case with many more product than reactant channels, which is common in ultracold experiments. In any case, Eq. (4) shows that the key factors that determine product-state distributions are the *relative* capture probabilities at different M .

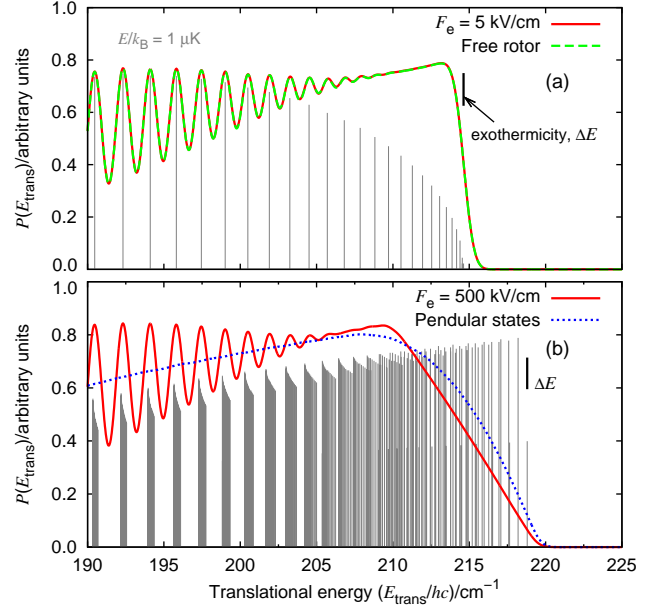


FIG. 2. (Color online) Statistical translational energy distributions for the ultracold reaction between ground-state ^{40}K and $^{87}\text{Rb}_2$ (red, solid) at: (a) low, and (b) high electric fields. The distributions for a free rotor (green, dashed) and pendular states (blue, dotted) are shown for comparison.

B. Statistical product distributions

Given the striking effect of external fields on ultracold reaction rates, it is of great interest to assess what effects can fields have on statistical product distributions. We focus on translational energy and rotational distributions for their practical interest, although the formalism can be applied to any observable of interest. In particular, translational energy distributions are likely to play an important role in the initial efforts to measure the products of ultracold reactions. At present, reaction experiments have low yields due to the limited number of reactants, thus translational distributions can be very valuable because they may provide information on the combined effect of various DOFs and do not require measuring products in nearly unpopulated states.

1. Control of statistical products

Figure 2 shows statistical translational energy distributions for the products of the ultracold reaction $^{40}\text{K} + ^{87}\text{Rb}_2 \rightarrow ^{40}\text{K}^{87}\text{Rb} + ^{87}\text{Rb}$ at relatively low/high values of an electric field, with reactants in their ground states. We focus on the behavior within 30 cm^{-1} of the maximum available kinetic energy and neglect nuclear spins to keep a manageable number of product states. The smooth curves are obtained by convoluting the calculated distributions (sharp peaks) with an “apparatus”

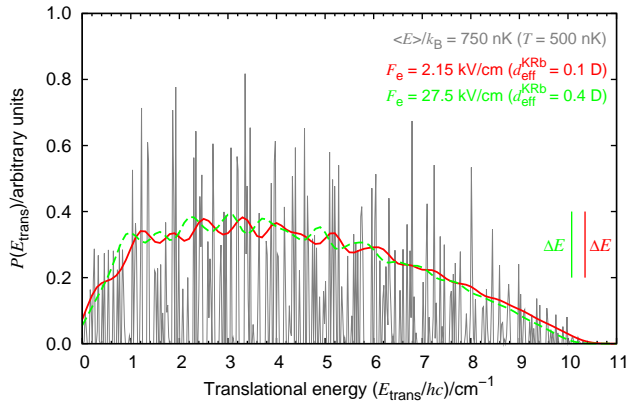


FIG. 3. (Color online) Statistical product translational energy distributions for the ultracold reaction $^{40}\text{K}^{87}\text{Rb} + ^{40}\text{K}^{87}\text{Rb} \rightarrow \text{K}_2 + \text{Rb}_2$, at different electric fields.

function (*i.e.*, Gaussian convolution), and are included to emphasize their overall shape. The factors determining the form of field-free statistical distributions have been previously studied [49]. The results in Fig. 2 indicate the degree of control over the *qualitative* form of product distributions that may be attained if fields act *directly* on the product energy levels. There are two main effects: (1) a change of the spectrum of product states which leads to a change of the *shape* of the distribution; and (2) a change of the reaction exothermicity. Such effects highlight the importance of accounting for fields when assessing the statistical nature of a reaction, given that statistical behavior may have different signatures at different field strengths.

Qualitative changes in statistical product distributions are mainly due to the modification of the product energy levels. For the $\text{K} + \text{Rb}_2$ reaction, such changes are most noticeable on a reduced energy range where rotational states are clearly resolved—which is why we restrict Fig. 2 to $v = 0$ states, even if $\text{KRb}(v = 0-2)$ products are energetically available. A similarly striking qualitative effect on vibrational distributions would require impractically high electric fields due to the relatively low electric dipole moment of KRb ; this is also why the fields needed for the strongest effects in the rotational states are very high. In general, the key factor determining the energy levels of a polar diatomic rotor is $d_{\text{eff}} F_e / B$ [50], where d_{eff} is the effective dipole moment, F_e the applied electric field and B the rotational constant. In principle, it is thus possible to tune the rotational distribution of such a product between those of a free rotor and pendular states simply by tuning the electric field.

Figure 3 shows statistical translational energy distributions for the prototypical reaction between two ground-state $^{40}\text{K}^{87}\text{Rb}$ molecules. Calculations include up to hyperfine terms. Vibrational excitation of the products is prevented because the exothermicity of the $\text{KRb} + \text{KRb}$ reaction is low, of about 10 cm^{-1} . In this case, products

are nonpolar species and the field act on the reactant states only. The main effect of the field is hence to shift the distributions by changing the reaction exothermicity, while preserving their qualitative behavior. In general, the exothermicity $\Delta E_\alpha \approx \max_\beta (E_\alpha - E_\beta)$ —given that $E \approx E_\alpha$ —may be increased or decreased with the applied field depending on whether reactants collide in a low-field-seeking or high-field-seeking state, which may in principle be used to fully suppress a reaction [34].

Both Figs. 2 and 3 show the control that is feasible on the statistical product distributions of prototypical reactions using electric fields. The effect of magnetic fields is different in two ways. First, large Zeeman splittings in paramagnetic species often require very high magnetic fields, thus the effects on reaction exothermicities and energy levels will be less pronounced than for polar species in electric fields. Secondly, magnetic fields lift all degeneracies and preserve total parity in the reaction, which may be used to restrict the product states that become available from specific initial reactant states. Effects due to this second feature will be most pronounced in cases where very few product states are energetically available.

2. Reaction mechanisms

So far, we assumed that interactions in the intermediate complex mix *all* DOFs considered, leading to a microcanonical distribution of *all* internal states. There exists, however, the possibility that some DOFs are much less involved and act as “spectators”, being adiabatically conserved during the reaction [51–53]. Such behavior would have a distinct signature in the calculated product distributions. Therefore, statistical distributions can aid distinguishing between different reaction mechanisms. Our formalism can be readily modified to explore these cases by restricting the sums to product states that fulfill the necessary constraints—also needed to account for the conservation of quantities other than M .

For instance, Mayle *et al.* [21] estimated nuclear spin-changing probabilities for typical ultracold reactions and predicted that hyperfine states are likely to change (be preserved) in processes involving heavier (lighter) species. Fig. 4 shows predicted rotational distributions for the products of the reaction of two ground-state $^{40}\text{K}^{87}\text{Rb}$ molecules in an electric field, where the *qualitative* differences between different schemes are clearly demonstrated. The oscillating pattern predicted if hyperfine DOFs are “active” during the reaction arise because the products are homonuclear Σ_g^+ -state molecules and exchange symmetry only allows even/odd values of the total nuclear spin for even/odd rotational states. A smooth distribution is predicted if nuclear spins are spectators. Both distributions extend to the same maximum rotational number, fixed by the total available energy. Statistical tests using predicted curves as *prior* distributions may be used to assess the involvement of different DOFs in a reaction, and its variation with varying conditions.

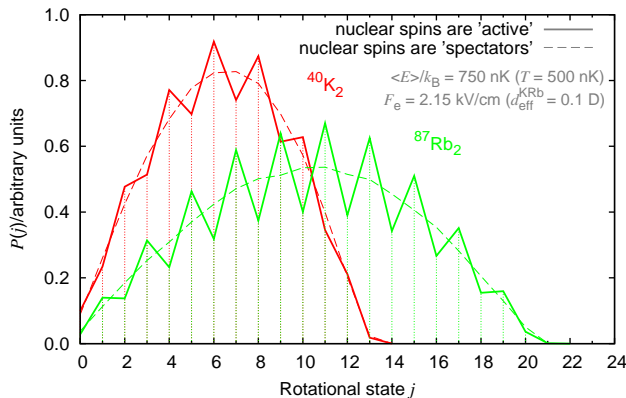


FIG. 4. (Color online) Statistical rotational distributions for the products $^{40}\text{K}_2$ (red) and $^{87}\text{Rb}_2$ (green) of the ultracold reaction between two ground-state $^{40}\text{K}^{87}\text{Rb}$ molecules in an electric field. Solid/dashed lines correspond to the case where nuclear spins are conserved/relaxed in the reaction.

IV. SUMMARY AND CONCLUSIONS

We have discussed a rigorous statistical formalism for determining state-to-state cross sections and product distributions in external fields. We show that external control of product distributions is possible, although limited, even for statistical reactions where the ultracold entrance channels are most “disconnected” from the products. We demonstrate how statistical predictions can be used to distinguish between different reaction mechanisms.

Product detection in ultracold reaction experiments is still very challenging. Current traps for neutrals are very shallow which makes in-trap measurements impractical, while out-of-trap detection is demanding because reactions have low yields due to the limited number of reactants. Several leading experimental groups are trying to achieve the higher densities of reactants that will be needed and developing new routes for product detection [19]. On the other hand, ionic products from ion-neutral or Penning-ionization reactions may be kept for long times using very deep traps and detected with highly-efficient techniques.

However, a thorough understanding of the physics driving ultracold reactions is ultimately conditioned by the advances that make possible the measurement of product-state distributions. For instance, information on the intermediate dynamics in ground-state collisions between reactive species (KRb , LiCs , *etc.*) may be useful in understanding/predicting the dynamics of similar intermediates in inelastic collisions between nonreactive species (RbCs , NaRb , *etc.*). In addition, experiments may explore reactions in mixed samples of homonuclear dimers such as $\text{Rb}_2 + \text{Cs}_2 \rightarrow 2\text{RbCs}$ in an attempt to better understand the inverse processes. All these considerations add to the relevance of alkali-metal dimers that are considered as less topical mostly because of their ground-state reactivity at ultracold temperatures [6, 8].

ACKNOWLEDGMENTS

The authors are grateful to Goulven Quémener and Piotr S. Żuchowski for discussions and comments on the manuscript. MLGM acknowledges funding from the 7th European research program FP7/2007-2013 under grant agreement No. 330623.

Appendix: Calculation details

This Appendix describes the calculation of quantum states and capture probabilities required for applying Eqs. (3) and (4) to the study of $^{40}\text{K} + ^{87}\text{Rb}_2 \rightarrow \text{KRb} + \text{Rb}$ and $^{40}\text{K}^{87}\text{Rb} + ^{40}\text{K}^{87}\text{Rb} \rightarrow \text{K}_2 + \text{Rb}_2$ reactions.

a. Quantum states

The Hamiltonian for the isolated alkali atoms, $^{40}\text{K}(^2\text{S})$ and $^{87}\text{Rb}(^2\text{S})$, is in general split into hyperfine and Zeeman contributions $\hat{\mathcal{H}} = \hat{\mathcal{H}}_{\text{hf}} + \hat{\mathcal{H}}_{\text{Z}}$. $\hat{\mathcal{H}}_{\text{hf}} = a \hat{i} \cdot \hat{s}$, with a the atomic hyperfine coupling constant, \hat{i} and \hat{s} the nuclear and electronic spin operators. $\hat{\mathcal{H}}_{\text{Z}} = g_{\text{S}} \mu_{\text{B}} \hat{s} \cdot \hat{F}_{\text{m}} - g_{\text{i}} \mu_{\text{N}} \hat{i} \cdot \hat{F}_{\text{m}}$, where $g_{\text{S}} \approx 2$ and g_{i} are the electron and nuclear g -factors, μ_{B} and μ_{N} the Bohr and nuclear magnetons, and \hat{F}_{m} the external magnetic field operator. The matrix elements for this Hamiltonian are taken from the literature, *cf.* Ref. [54]. Quantum states are calculated from the diagonalization of the resulting Hamiltonian matrix for a specific value of the external fields, using the parameters from NIST atomic database [36].

The quantum states for $^{40}\text{K}_2(^1\Sigma_g^+)$, $^{87}\text{Rb}_2(^1\Sigma_g^+)$ and $^{40}\text{K}^{87}\text{Rb}(^1\Sigma^+)$, in their vibrational ground states, are computed using the formalism in Refs. [37, 38]. In general, the molecular Hamiltonian is split into rotational, hyperfine, Zeeman and Stark terms as $\hat{\mathcal{H}} = \hat{\mathcal{H}}_{\text{rot}} + \hat{\mathcal{H}}_{\text{hf}} + \hat{\mathcal{H}}_{\text{Z}} + \hat{\mathcal{H}}_{\text{S}}$, which read

$$\begin{aligned} \hat{\mathcal{H}}_{\text{rot}} &= B\hat{n}^2 - D\hat{n}^2\hat{n}^2, \\ \hat{\mathcal{H}}_{\text{hf}} &= \sum_{k=1}^2 \hat{V}_k : \hat{Q}_k + \sum_{k=1}^2 c_k \hat{n} \cdot \hat{i}_k + c_3 \hat{i}_1 \cdot \mathbf{T} \cdot \hat{i}_2 + c_4 \hat{i}_1 \cdot \hat{i}_2, \\ \hat{\mathcal{H}}_{\text{Z}} &= -g_{\text{r}} \mu_{\text{N}} \hat{n} \cdot \hat{F}_{\text{m}} - \sum_{k=1}^2 g_k \mu_{\text{N}} \hat{i}_k \cdot \hat{F}_{\text{m}} (1 - \sigma_k), \\ \hat{\mathcal{H}}_{\text{S}} &= -\hat{d} \cdot \hat{F}_{\text{e}}. \end{aligned} \quad (\text{A.1})$$

Here, \hat{n} is the operator of the rotational angular momentum, while \hat{i}_k ($k = 1, 2$) are those of the nuclear spins of the individual atoms. B and D are the rotational and centrifugal distortion constants (we neglect the latter, following Refs. [37, 38]). The first term in the hyperfine Hamiltonian corresponds to the interaction of the electric quadrupole moment of each nucleus, Q_k , with the electric field gradient it experiences, V_k . The other three hyperfine terms correspond to the nuclear-spin rotation for each nucleus (with associated coupling constants c_1

and c_2), the tensor (c_3) and scalar (c_4) interactions between the nuclear spins. T is a tensor describing the angular dependence of the direct spin-spin interaction and the anisotropic part of the indirect spin-spin interaction [55]. The Zeeman Hamiltonian involves a rotation term with rotation g -factor g_r , and nuclear terms including the isotropic part of the nuclear shielding tensor, σ . The Stark Hamiltonian is only relevant for KRb, and involves the electric dipole moment \hat{d} and electric field \hat{F}_e operators. All matrix elements are given in the appendices of Refs. [37, 38]; the molecular parameters for $^{40}\text{K}_2$ and $^{87}\text{Rb}_2$ are reported in Table I of Ref. [38], while those for $^{40}\text{K}^{87}\text{Rb}$ are in Table V of Ref. [37].

Only $^{40}\text{K}_2(^1\Sigma_g^+, v=0)$ and $^{87}\text{Rb}_2(^1\Sigma_g^+, v=0)$ products are populated in the KRb+KRb reaction, with a zero-field exothermicity of -10.355 cm^{-1} [1]. The zero-field exothermicity of the $^{40}\text{K}+^{87}\text{Rb}_2$ reaction is -214.617 cm^{-1} [1], and does not exceed -220 cm^{-1} for the electric fields considered. Hence, only vibrational states $v=0-2$ of the KRb products are energetically accessible [56]. For the latter reaction, we neglect the couplings between states corresponding to different vibrational manifolds and the variation of molecular con-

stants with the vibrational state v . Different vibrational states are added a vibrational energy of $E_{\text{vib}} = \hbar w(v + \frac{1}{2})$, with $w = 75.85 \text{ cm}^{-1}$ for KRb [56].

b. Capture probabilities

Three different capture models were used in the calculations, two quantum models for the capture of ultracold reactants: (1) a WKB approximation for collisions in magnetic fields, and (2) the adiabatic variant of QTM by Quémener and Bohn [10] for collisions in electric fields; and one for the capture of products: (3) a semiclassical model based on PST [39–42].

In our calculations, we approximate the capture probabilities for the ultracold reactants by the tunneling probability through dynamical barriers in the entrance channels. All dispersion coefficients are taken from *ab initio* data [57, 58]

WKB capture model. The capture probability is calculated using the WKB expression for the transmission probability through a centrifugal barrier

$$p_\gamma^M(E, F_m) = \exp \left\{ -\frac{2}{\hbar} \int_{R_{\min}}^{R_{\max}} \sqrt{2\mu_\gamma \left[\frac{L_\gamma(L_\gamma + 1)\hbar^2}{2\mu_\gamma R^2} - \frac{C_{6,\gamma}}{R^6} - (E - E_\gamma) \right]} dR \right\}, \quad (\text{A.2})$$

where R_{\min} and R_{\max} are the classical turning points (zeroes of the factor within square brackets), which are determined numerically. μ_γ and $C_{6,\gamma}$ are the relevant reduced mass and long-range dispersion coefficient, while L_γ is the orbital angular quantum number. The dependence of this probability with the applied magnetic field, F_m , arises from that of E_γ (and thus of R_{\min} and R_{\max}).

QTM capture model. The model was developed by Quémener and Bohn [10] to account for the strong effect of the electric dipole-dipole interaction on the dynamical barriers. The capture probability is calculated from their model for the transition probability, Eq. (14) in Ref. [10],

$$p_\gamma^M(E, F_e) = q \times \left(\frac{E - E_\gamma}{V_{b,\gamma}} \right)^{L_\gamma + 1/2}, \quad (\text{A.3})$$

where $q \approx 2/3$ is a correction factor and $V_{b,\gamma}$ the height of the dynamical barrier [2, 10]. In this case, the dependence on the electric field F_e arises from that of $V_{b,\gamma}$. The barrier height is obtained from the diagonalization of the long-range interaction including the electric dipole-dipole term. In the orbital angular momentum basis, the matrix

elements read

$$\begin{aligned} &\langle L_\gamma M_{L_\gamma} | V(R) | L'_\gamma M_{L'_\gamma} \rangle \\ &= \delta_{L_\gamma, L'_\gamma} \left[\frac{\hbar^2 L_\gamma(L_\gamma + 1)}{2\mu_\gamma R^2} - \frac{C_{6,\gamma}}{R^6} \right] - \frac{C_{3,\gamma}}{R^3}, \end{aligned} \quad (\text{A.4})$$

with

$$\begin{aligned} C_{3,\gamma} &= 2d_{\text{eff},1}^\gamma d_{\text{eff},2}^\gamma (-1)^{M_{L_\gamma}} [(2L_\gamma + 1)(2L'_\gamma + 1)]^{1/2} \\ &\times \begin{pmatrix} L_\gamma & 2 & L'_\gamma \\ 0 & 0 & 0 \end{pmatrix} \begin{pmatrix} L_\gamma & 2 & L'_\gamma \\ -M_{L_\gamma} & 0 & M_{L'_\gamma} \end{pmatrix}, \end{aligned} \quad (\text{A.5})$$

where $d_{\text{eff},k}^\gamma$ ($k=1,2$) are the effective/induced electric dipole moments for each species and $(:::)$ represents a Wigner 3- j symbol. The barrier height $V_{b,\gamma}$ is the smallest eigenvalue of the matrix defined by Eq. (A.4), which is diagonalized for each M_{L_γ} (M) using $L_\gamma = 1, 3, \dots, 9$.

PST capture model. This model is used for capture in the product channels only, where the kinetic energy is relatively large and the effect of a few near-threshold states below dynamical barriers may be neglected. The capture probabilities are computed as

$$p_\gamma^M(E, F) = \begin{cases} 1, & \text{if } E - E_\gamma \geq V_{b,\gamma} \\ 0, & \text{otherwise,} \end{cases} \quad (\text{A.6})$$

where the height of the centrifugal barrier is

$$V_{b,\gamma} = \sqrt{\frac{[L_\gamma(L_\gamma + 1)\hbar^2]^3}{54\mu_\gamma^3 C_{6,\gamma}}}. \quad (\text{A.7})$$

p_γ^M dependence on the field(s) arises from that of E_γ .

-
- [1] S. Ospelkaus, K.-K. Ni, D. Wang, M. H. G. de Miranda, B. Neyenhuis, G. Quémener, P. S. Julienne, J. L. Bohn, D. S. Jin, and J. Ye, *Science* **327**, 853 (2010).
- [2] K.-K. Ni, S. Ospelkaus, D. Wang, G. Quémener, B. Neyenhuis, M. H. G. de Miranda, J. L. Bohn, J. Ye, and D. S. Jin, *Nature* **464**, 1324 (2010).
- [3] M. H. G. de Miranda, A. Chotia, B. Neyenhuis, D. Wang, G. Quémener, S. Ospelkaus, J. L. Bohn, J. Ye, and D. S. Jin, *Nat. Phys.* **7**, 502 (2011).
- [4] R. V. Krems, *Phys. Chem. Chem. Phys.* **10**, 4079 (2008).
- [5] D. J. Nesbitt, *Chem. Rev.* **112**, 5062 (2012).
- [6] P. S. Żuchowski and J. M. Hutson, *Phys. Rev. A* **81**, 060703 (2010).
- [7] J. N. Byrd, J. A. Montgomery, and R. Côté, *Phys. Rev. A* **82**, 010502 (2010).
- [8] M. Tomza, K. W. Madison, R. Moszynski, and R. V. Krems, *Phys. Rev. A* **88**, 050701 (2013).
- [9] B. Zhu, B. Gadway, M. Foss-Feig, J. Schachenmayer, M. L. Wall, K. R. A. Hazzard, B. Yan, S. A. Moses, J. P. Covey, D. S. Jin, et al., *Phys. Rev. Lett.* **112**, 070404 (2014).
- [10] G. Quémener and J. L. Bohn, *Phys. Rev. A* **81**, 022702 (2010).
- [11] G. Quémener and J. L. Bohn, *Phys. Rev. A* **81**, 060701(R) (2010).
- [12] Z. Idziaszek and P. S. Julienne, *Phys. Rev. Lett.* **104**, 113202 (2010).
- [13] Z. Idziaszek, G. Quémener, J. L. Bohn, and P. S. Julienne, *Phys. Rev. A* **82**, 020703 (2010).
- [14] K. Jachymski, M. Krych, P. S. Julienne, and Z. Idziaszek, *Phys. Rev. Lett.* **110**, 213202 (2013).
- [15] B. Gao, *Phys. Rev. Lett.* **105**, 263203 (2010).
- [16] B. Gao, *Phys. Rev. A* **83**, 062712 (2011).
- [17] F. H. J. Hall, M. Aymar, N. Bouloufa-Maafa, O. Dulieu, and S. Willitsch, *Phys. Rev. Lett.* **107**, 243202 (2011).
- [18] J. Jankunas, B. Bertsche, K. Jachymski, M. Hapka, and A. Osterwalder, *J. Chem. Phys.* **140**, 244302 (2014).
- [19] A. Härter, A. Krülov, M. Deisz, B. Drews, E. Tiemann, and J. H. Denschlag, *Nat. Phys.* **9**, 512 (2013).
- [20] T. V. Tscherbul and R. V. Krems, *J. Chem. Phys.* **129**, 034112 (2008).
- [21] M. Mayle, B. P. Ruzic, and J. L. Bohn, *Phys. Rev. A* **85**, 062712 (2012).
- [22] M. Mayle, G. Quémener, B. P. Ruzic, and J. L. Bohn, *Phys. Rev. A* **87**, 012709 (2013).
- [23] A. Frisch, M. Mark, K. Aikawa, F. Ferlaino, J. L. Bohn, C. Makrides, A. Petrov, and S. Kotochigova, *Nature* **507**, 475 (2014).
- [24] W. Hauser and H. Feshbach, *Phys. Rev.* **87**, 366 (1952).
- [25] W. H. Miller, *J. Chem. Phys.* **52**, 543 (1970).
- [26] R. V. Krems, B. Friedrich, and W. C. Stwalley, eds., *Cold Molecules: Theory, Experiment, Applications* (Taylor & Francis, London, 2009), ISBN 978-1-4200-5903-8.
- [27] R. D. Levine, *Molecular Reaction Dynamics* (Cambridge University Press, Cambridge, 2005).
- [28] A. A. Buchachenko, *Moscow Univ. Chem. Bull.* **67**, 159 (2012).
- [29] A. A. Buchachenko, A. V. Stolyarov, M. M. Szcześniak, and G. Chałasiński, *J. Chem. Phys.* **137**, 114305 (2012).
- [30] E. J. Rackham, F. Huarte-Larranaga, and D. E. Manolopoulos, *Chem. Phys. Lett.* **343**, 356 (2001).
- [31] T. González-Lezana, *Int. Rev. Phys. Chem.* **26**, 29 (2007).
- [32] H. Guo, *Int. Rev. Phys. Chem.* **31**, 1 (2012).
- [33] M. L. González-Martínez, L. Bonnet, and P. Larrégaray (2014), in preparation.
- [34] E. R. Meyer and J. L. Bohn, *Phys. Rev. A* **82**, 042707 (2010).
- [35] J. F. E. Croft and J. L. Bohn, *Phys. Rev. A* **89**, 012714 (2014).
- [36] *NIST: Basic atomic spectroscopic data* (2014).
- [37] J. Aldegunde, B. A. Rivington, P. S. Żuchowski, and J. M. Hutson, *Phys. Rev. A* **78**, 033434 (2008).
- [38] J. Aldegunde and J. M. Hutson, *Phys. Rev. A* **79**, 013401 (2009).
- [39] J. C. Light, *J. Chem. Phys.* **40**, 3221 (1964).
- [40] P. Pechukas and J. C. Light, *J. Chem. Phys.* **42**, 3281 (1965).
- [41] E. E. Nikitin, *Teor. Eksp. Khim. Akad. Nauk. Ukr. SSR* **1**, 135 (1965).
- [42] C. Klotz, *J. Phys. Chem.* **75**, 1526 (1971).
- [43] P. Larrégaray, L. Bonnet, and J.-C. Rayez, *J. Phys. Chem. A* **110**, 1552 (2006).
- [44] P. Bargueño, T. González-Lezana, P. Larrégaray, L. Bonnet, and J.-C. Rayez, *Phys. Chem. Chem. Phys.* **9**, 1127 (2007).
- [45] P. Bargueño, T. González-Lezana, P. Larrégaray, L. Bonnet, J.-C. Rayez, M. Hankel, S. C. Smith, and A. J. H. M. Meijer, *J. Chem. Phys.* **128**, 244308 (2008).
- [46] F. Dayou, P. Larrégaray, L. Bonnet, J.-C. Rayez, P. Nilo Arenas, and T. González-Lezana, *J. Chem. Phys.* **128**, 174307 (2008).
- [47] M. Jorfi, P. Honvault, P. Bargueño, T. González-Lezana, P. Larrégaray, L. Bonnet, and P. Halvick, *J. Chem. Phys.* **130**, 184301 (2009).
- [48] F. J. Aoiz, V. Sáez-Rábanos, T. González-Lezana, and D. E. Manolopoulos, *J. Chem. Phys.* **126**, 161101 (2007).
- [49] L. Bonnet and J.-C. Rayez, *Phys. Chem. Chem. Phys.* **1**, 2383 (1999).
- [50] K. Von Meyenn, *Z. Physik* **231**, 154 (1970), in German.
- [51] M. Quack and J. Troe, *Ber. Bunsenges Phys. Chem.* **78**, 240 (1974).
- [52] R. A. Marcus, *J. Chem. Phys.* **62**, 1372 (1975).
- [53] G. Worry and R. A. Marcus, *J. Chem. Phys.* **67**, 1636 (1977).
- [54] M. L. González-Martínez and J. M. Hutson, *Phys. Rev. A* **88**, 053420 (2013).
- [55] D. L. Bryce and R. E. Wasylshen, *Acc. Chem. Res.* **36** (2003).
- [56] C. Amiot and J. Vergès, *J. Chem. Phys.* **112** (2000).
- [57] P. S. Żuchowski, M. Kosicki, M. Kodrycka, and P. Soldán, *Phys. Rev. A* **87**, 022706 (2013).
- [58] M. Kosicki and P. S. Żuchowski (2014), private communication.